Speciation of chromium on a straw lignin: adsorption isotherm, EPR, and XAS studies

Karine Flogeac,[a] Emmanuel Guillon,*[a] Eric Marceau[b] and Michel Aplincourt[a]

[a] *GRECI (Groupe de Recherche En Chimie Inorganique), Université de Reims Champagne-Ardenne, BP 1039, 51687, Reims Cedex 2, France. E-mail: emmanuel.guillon@univ-reims.fr; Fax: +33 (0) 3 26 91 32 43 Tel: +33 (0) 3 26 91 31 42*

[b] *Laboratoire de Réactivité de Surface, Université Pierre et Marie Curie, UMR CNRS 7609, 4 place Jussieu, 75252, Paris Cedex 05, France*

Received (in London, UK) 18th November 2002, Accepted 30th January 2003
First published as an Advance Article on the web 5th March 2003

The binding ability of a lignocellulosic substrate extracted from wheat straw with chromium(III) ion was investigated. The study was carried out at macroscopic and microscopic scales. The adsorbent used was first characterised using X-ray diffraction and electron microscopy. Then, macroscopic studies were conducted using batch adsorption experiments, at room temperature, as a function of time, pH, and metal concentration. The results obtained indicate that several successive phenomena take place at the substrate surface. Indeed, sorption, co-precipitation, and precipitation processes arise depending on the experimental conditions. The speciation of Cr was also investigated, at the atomic scale, by EPR, extended X-ray absorption fine structure (EXAFS), and X-ray absorption near edge structure (XANES). This study revealed that chromium(III) surface complexes have an octahedral geometry. Chromium ions are held in inner-sphere complexes, and are coordinated to six oxygen atoms at an average distance of 1.90 Å.

Introduction

In the last decade, there has been a growing awareness of the necessity to protect our environment in order to guarantee the long term development of our societies. Molecular environmental science is a recent discipline, which aims at understanding the fundamental properties and reactivities of natural organic and inorganic systems in order to match scientific answers to environmental issues. The case of the pollution of soils and biota by toxic metals is one of the most important ones. The release of toxic metals in the environment, and specifically in soils and industrial or domestic urban waste, endangers living organisms. The toxicity of an element primarily depends on its chemical form at the atomic scale, or speciation, because this form determines its solubility, which itself controls its mobility and, ultimately, the capacity of this element to enter cells. For this reason, determining the form of pollutants is essential to assess the risk associated with their presence, and a prerequisite to the design of cost-effective and efficient recovering techniques, and to prevent future contamination in the case of landfills. The notion of speciation is taken in a broad sense, and includes complexation surface parameters of toxic metals (pH, time, ionic strength, and concentration) as well as the electronic configuration and structural chemistry of these metals.

Lignin is a major component of plants where it serves as a binding agent for cellulose and other materials. Consequently, lignin is found in great abundance in soils. The structure of lignin is rather complex. It is a polymer of coniferin, which contains propane units having aldehyde, keto, hydroxy, methoxy, and phenolic groups.[1] The acido-basic treatment of wheat straw, in order to obtain insoluble lignocellulosic substrate (LS), produces polyhydroxy phenolic, and carboxylic acid functional groups.[1–3] In recent years, some progress have been made in determining the ability of this material to sorb toxic metals.[4–7] Very few results are available about chromium sorption on lignin materials and yet higher allowable concentrations of this metal have been detected in ground soil and ground water. Chromium is present in aqueous solutions mainly in two oxidation states, Cr(III) and Cr(VI). Depending on its oxidation state, Cr can be either toxic or beneficial.[8–10] Water soluble Cr(VI) is extremely irritating and toxic to human body tissue owing to its oxidising potential and easy permeation of biological membranes.[11]

Chromium in its trivalent form is an essential trace element for plants and animals; it is involved in glucose metabolism and nucleic acid synthesis.[12] However, Cr(III) has also been shown to a potential hazard, especially in the aquatic environment. Indeed, *in vitro* tests have shown that trivalent chromium is a potential toxin, because it is a competitive inhibitor of many cellular processes.[13] The main sources of Cr pollution are mines, leather tanneries, the cement industry, as well as its use in dyes, electroplating, production of steel, photographic materials, and corrosive paints.[14] The principal techniques for recovering or removing Cr from wastewater are chemical reduction and precipitation, adsorption by several types of adsorbents such as lignin materials. Therefore, there is a great need for the understanding of sorption processes, which requires knowledge of the electronic and structural parameters.

The main objective of this study is to evaluate the binding ability of a lignin material in order to quantify the sorption phenomenon compared with the chromium passage in groundwater. First, characterisation of LS by X-ray diffraction (XRD), transmission electron microscopy (TEM) experiments, and energy dispersive X-ray spectrometry (EDX) analysis is done. Then, the parameters governing the sorption processes are determined. Finally, the chromium surface complexes

 DOI: 10.1039/b211411a

geometry and structure are studied by electronic paramagnetic resonance (EPR) and X-ray absorption (XAS) spectroscopies.

Experimental

KNO_3, HNO_3, and KOH were obtained in the purest commercially available grade (*puriss*) and used without further purification. The metal ion stock solutions were prepared from chromium(III) nitrate *puriss* reagent (Fluka).

Substrate preparation

The LS (Lignocellulosic Substrate) powder was obtained after successive acido-basic treatments of wheat straw, in order to eliminate soluble molecules such as sugars, hemicellulose, and low molecular weight lignin molecules.[15] As a consequence, the resulting powder is quasi-insoluble in the pH range 2–10 (DOC values $\ll 1\%$). The solid was air-dried and ground to pass a 100 μm sieve.

Adsorption experiments

The sorption studies as a function of pH were conducted using batch experiments at 293 K. The LS substrate (2 g L^{-1}) was immersed in 15 mL of 0.1 mol L^{-1} KNO_3 solution and stirred for one day, which corresponds to the hydration time of the solid. Then, chromium(III) was added at the concentration of 1×10^{-4} mol L^{-1}, and the pH was adjusted to a fixed value by adding 0.1 mol L^{-1} HNO_3 or 0.1 mol L^{-1} KOH. The final volume was adjusted to 25 mL. The sorption equilibrium was predetermined by kinetic experiments in which different contact times between the metal and the solid were applied. The flasks were then shaken at 293 K for 12 hours with an automatic shaker to ensure complete sorption. After filtration through a 0.20 μm polyamide membrane, the unsorbed metal ion concentration was measured by a Varian ICP-AES spectrometer and the quantity of sorbed chromium was deduced from the initial concentration. Adsorption isotherms were carried out in the same way at a fixed pH value equal to 4.80 and with chromium concentrations ranging from 10 to 3000 μmol L^{-1}.

XRD and TEM–EDX studies

Powder X-ray diffraction (XRD) measurements were performed at room temperature between $2\theta = 5$ and 55° on a Siemens D500 diffractometer, using the Kα radiation of copper (1.5418 Å).

Transmission electron microscopy (TEM) experiments were performed on a 100 kV JEOL 100 CXII UHR microscope. Scanning TEM–EDX analyses were obtained on a 200 kV JEOL JEM 2010 microscope equipped with a PGT Imix PC X-ray emission spectrometer and a Si(Li) detector. After grinding of the sample, the powder was dispersed in pure ethanol. The suspension was stirred in an ultrasonic bath and one drop was placed on a carbon-coated copper grid.

EPR experiments

The solid state EPR spectrum was obtained with a Brüker ELEXYS 500 spectrometer operating at X-band frequency with a 100 kHz modulation frequency. The spectrum was recorded under the following conditions: microwave power: 1 mW, modulation amplitude: 4 G. The spectrum was recorded at 77 K.

X-Ray absorption data collection and processing

The XANES and EXAFS spectra were collected at the Laboratoire d'Utilisation du Rayonnement Electromagnétique (LURE), Paris-Sud University, on the storage ring DCI with an energy of 1.85 GeV and a mean intensity of 300–200 mA. The measurements were carried out at the chromium K-edge in the fluorescence mode at the XAS-4 station. The monochromator used was a Si(111) for EXAFS or a Si(311) for XANES channel-cut, which was detuned to 50% of the maximal intensity to remove the higher-order harmonics. The detectors were low-pressure (≈0.2 atm) air-filled ionisation chambers. The spectra were the sum of ten recordings in the range 5840–7000 eV for EXAFS, including the chromium K-edge (≈5989 eV). The photon energy was calibrated from the spectrum of a chromium foil, assigning 5989 eV to the pre-edge peak. Spectra were recorded using sampling steps of 0.3 eV (XANES) and 2 eV (EXAFS), an integration time of 2.0 s per point was used in both cases. The EXAFS data analysis was performed with the "EXAFS pour le Mac" and EXAFS98 programs.[16] This standard EXAFS analysis[17] includes linear pre-edge background removal, polynomial atomic absorption calculation (of order 5), Lengeler–Eisenberger EXAFS spectra normalisation,[18] and reduction from the absorption data $\mu(E)$ to the EXAFS spectrum $\chi(k)$. Radial distribution functions $F(R)$ were calculated by Fourier transforms of $k^3 w(k)\mu(k)$ in the range 2–13 $Å^{-1}$; $w(k)$ is a Kaiser–Bessel apodisation window with a smoothness coefficient $\tau = 2.5$. After Fourier filtering, the first shell Cr–6O is fitted, in the range 2–13 $Å^{-1}$ to the standard EXAFS formula, without multiple scattering:

$$\chi(k) = S_0^2 \sum_i \left[\frac{N_i}{R_i^2} A_i(k) e^{-2\sigma_i^2 k^2} e^{-2R_i/\lambda_i(k)} \sin(2kR_i + \Phi_i(k)) \right]$$

We used $i = 1$ and $N_i = 6$, and the experimental phase, $\Phi_i(k)$, and amplitude, $A_i(k)$, were extracted from the model compounds $K_3[Cr(C_2O_4)_3]\cdot 3H_2O$, $Cr(H_2O)_6^{3+}$, and $Cr(acac)_3$.

Results and discussion

Characterisation of LS

LS was analysed by various techniques[3] and it is composed of 25% lignin and 75% cellulose. Briefly, acid group amounts, likely involved in complexation and determined by IR and ^{13}C-CP/MAS NMR spectroscopies, were estimated by potentiometric titrations: carboxylic and phenolic moieties were found to be equal respectively to 0.24 mmol g^{-1} and 0.80 mmol g^{-1}. The specific surface area (196 m^2 g^{-1}) was determined from an aqueous vapor adsorption isotherm, using the BET method to approximate the wet-solid conditions in a better way. Moreover, a tiny amount of silicon was found. In order to characterise this phase, the residue obtained after nitric acid attack of LS, as a white powder, was analysed. It was identified as silica by two intense EDX peaks at 0.523 and 1.740 keV corresponding to the oxygen and silicon K lines, respectively. Silica has been reported to be a constituent of grass (*Poaceae*) shoots such as oat or rice.[19] Transmission electron microscopy carried out on the residue showed the presence of two distinct morphologies, large homogeneous spheres (> 0.1 μm) (Fig. 1a) and more heterogeneous zones formed by small entities organised in larger spherical groups or linear spindles (Fig. 1b).

To our knowledge, the powder X-ray diffractogram of LS (Fig. 2) has never been presented in the literature. It can be discussed on the basis of reference compounds, corresponding to each of its constituents.

Lignin gives a broad diffraction halo with a maximum at about $2\theta = 20°$, superimposed with less intense sharper peaks, which is in agreement with Rohella *et al.*[20] The diffractogram of the siliceous residue obtained after acidic treatment contains one broad band at $2\theta = 22.2°$. The silica is not well crystallised and this may correspond to an opal-A_G type, *i.e.* hydrated gel-like silica composed of spherical structures, a feature that

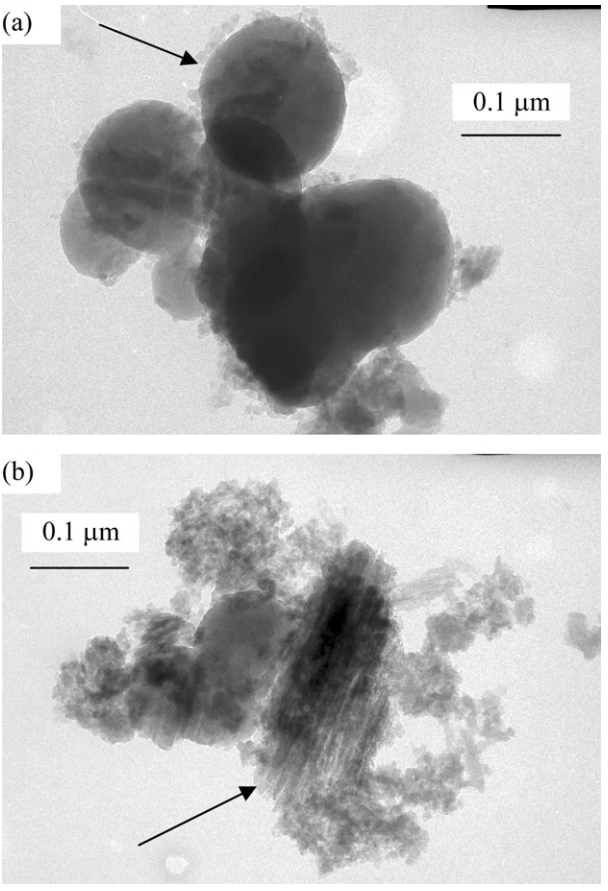

Fig. 1 TEM micrographs from the siliceous residue obtained after acidic treatment: (a) large spheres; (b) small spheres and linear spindle-like (→) morphology.

distinguishes it from silica glass.[21] It must be noted that the acidic treatment could have modified the crystallinity of silica compared with its state in the initial LS. Silica in *Poacea* shoots such as bamboo[22] is reported to be of the opal-CT ("cristobalite-like") type, giving an intense diffraction line at $2\theta = 22.2°$ and a smaller one around 36°.[21] Opal-CT is more organised than opal-A_G and occurs as aggregates of thin blades or fibers, which resembles the spindle-like organisation seen by TEM.[23] Finally, a sample of pure cellulose, giving the same NMR and X-ray photoelectron spectroscopy signals as LS,[24] was studied as a reference. It exhibited three diffraction lines, in agreement with Abou-Sekkina *et al.*[25] (JCPDS 50-2241) and Deraman *et al.*[26] in terms of position and relative intensities: a broad asymmetric peak at $2\theta = 15°$, corresponding to amorphous cellulose, a sharp peak at $2\theta = 22.6°$, and a small peak at 34°, corresponding to crystalline cellulose.

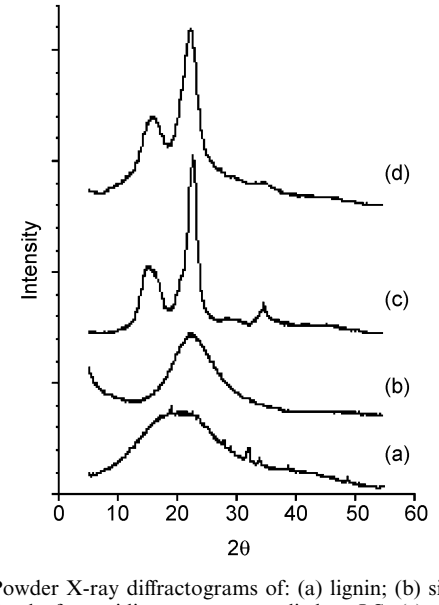

Fig. 2 Powder X-ray diffractograms of: (a) lignin; (b) siliceous residue obtained after acidic treatment applied to LS; (c) cellulose; (d) non-treated LS.

Three diffraction lines were observed on the LS diffractogram. The one at $2\theta = 16°$ comes from the amorphous fraction of cellulose, implying that the two other peaks at 22.2 and 34° contained at least strong contributions from crystalline cellulose. However, the presence of opal-CT in LS could not be discarded since its diffraction peaks would be found at about the same positions as the peaks of crystalline cellulose. Indeed, a non-negligible contribution from opal-CT could account for the localisation of the second peak at 22.2° instead of 22.6° for cellulose. Lignin seems to provide only a minor contribution to the diffractogram. It might explain the broadening observed below 15°, absent from the cellulose diffractogram.

We have shown in previous work[7,15] that only lignin is implicated in the sorption process. Cellulose, which does not present potential coordination binding sites, and silica, which is in negligible quantity, are not involved in the process of adsorption.

Adsorption experiments

Kinetic experiments were preliminarily carried out to determine and evaluate the equilibrium time of the complexation reaction between Cr(III) and LS. The kinetics of trivalent chromium sorption were studied by varying the contact time from 5 min to 48 h using 2 g L^{-1} of LS and an initial metal concentration of 1×10^{-4} mol L^{-1} (Fig. 3). The metal sorption takes place in two steps. The first one involves fast uptake within the first three hours of contact and is followed by a much slower gradual uptake that may continue for days. This result agrees with several previous studies on Cr(III) sorption.[27–29] Several mechanisms have been postulated to explain these two steps, and this slow uptake.[30,31] The most likely is that in the first hours of sorption an equilibrium between the adsorbed metal amount and the metal ion amount in solution is already attained (fast process). Then, the formation of polynuclear complexes, diffusion into LS, and surface precipitation could occur. In order to limit these phenomena, and for practical reasons, we chose to carry out our experiments with an equilibrium time equal to 12 hours, which also ensures the completion of the fast sorption step. Moreover, the second step is still negligible, compared to the first one, in chromium sorption terms.

The effect of solution pH on the adsorption of Cr(III) is shown in Fig. 4. Adsorption of Cr(III) is strongly dependent

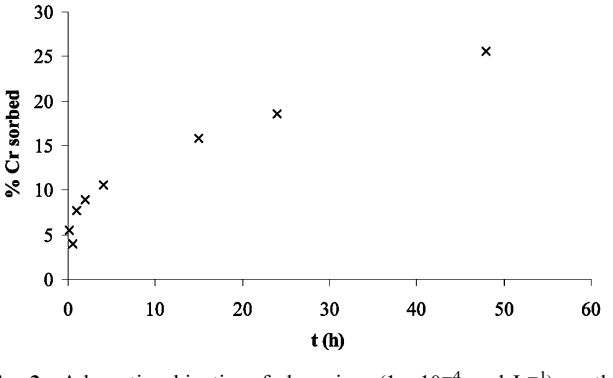

Fig. 3 Adsorption kinetics of chromium (1×10^{-4} mol L^{-1}) on the LS (2 g L^{-1}) in 0.1 M KNO_3 at pH 4.80.

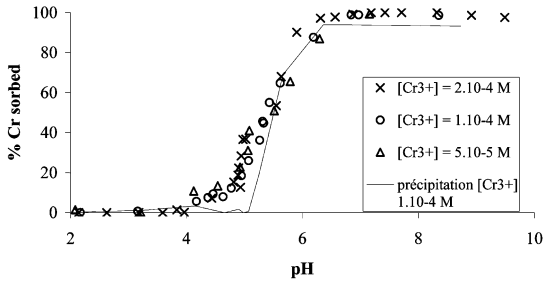

Fig. 4 Chromium adsorption on LS (2 g L^{-1}) as a function of pH for various Cr^{3+} concentration at 293 K in 0.1 M KNO_3.

on pH. Adsorption increases with pH, the maximum sorption being reached between pH 6 and 7. Fig. 4, with increasing chromium concentration, shows that a lower solid/Cr(III) ratio leads to a slight shift of the pH edge to higher pH. Moreover, the two curves with higher Cr(III) concentrations seem to present a break in the pH edge around pH = 5. This break corresponds to chromium hydroxide precipitation. Indeed, chromium precipitation ($Cr(OH)_3$) occurs around pH = 5 for 1×10^{-4} and 2×10^{-4} mol L^{-1} concentrations. Moreover, polymeric species of chromium(III) hydroxide such as $Cr_2(\mu\text{-}OH)_2(OH)_4(OH_2)_4$ can become predominant at this pH value and metal concentration.[32,33] Fig. 4 clearly shows that metal sorption takes place before precipitation until pH = 5.2. So, in order to avoid metal hydrolysis processes at the LS surface, a pH of 4.8 was chosen for isotherm experiments as a function of the metal concentration. Indeed, from pH 5.2 upwards, sorption and precipitation seem to be superimposed (Fig. 4). The reversibility of the sorption of Cr(III) ions onto LS has been studied between pH 2.0 and 8.0, and revealed a relatively weak desorbed amount, *i.e.* ~10%, as previously shown by Csoban *et al.*[30]

The sorption isotherm of Cr(III) ions onto LS at pH 4.80 is given in Fig. 5. This isotherm seems to be subdivided into three regions. In the low concentration region ($\leq$150 µmol g^{-1}) the amount of metal sorbed is proportional to the metal ion concentration introduced, and represents at least 34% of the total Cr(III). At higher concentration (200 µmol $g^{-1} \leq [Cr^{3+}] \leq 600$ µmol g^{-1}), the adsorption curves presents an inflection point and a decrease in slope around this point. This part of the curve corresponds to a co-precipitation phenomenon (*i.e.* sorption and precipitation simultaneously). At larger total Cr(III) concentrations, the amount of metal sorbed increases again, in proportion to the concentration of chromium ion introduced corresponding to surface precipitation. From this curve,

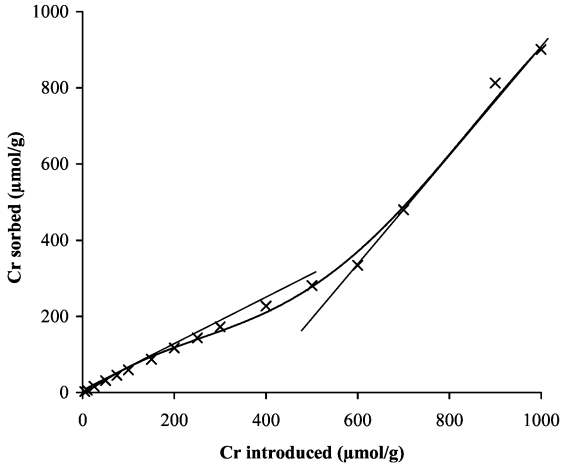

Fig. 5 Cr^{3+} adsorption isotherm on LS (2 g L^{-1}) at pH 4.80.

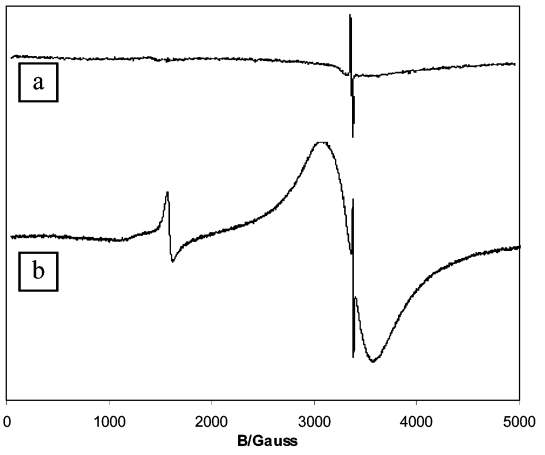

Fig. 6 EPR spectrum of LS alone (a), and the Cr–LS system (b) at 77 K ($[Cr^{3+}]$ = 50 µmol g^{-1}, pH 4.80).

the Cr^{3+} ion amount sorbed onto LS can be estimated, even if the curve does not present a plateau. Indeed, at a chromium concentration introduced equal to 150 µmol g^{-1}, 87 µmol g^{-1} of Cr(III) are sorbed, which corresponds to 4.52 mg g^{-1}. These results are in accordance with those found by Charlet and Manceau[34] for sorption of Cr(III) by hydrous Fe oxides. After the macroscopic properties of chromium sorption onto LS, microscopic studies of the surface complexes were carried out using EPR and XAS spectroscopies. The chromium(III)–LS solid for these analyses was obtained by stirring a weighed amount (50 mg) of LS with metal solution (1×10^{-4} mol L^{-1}) at pH 4.80 for EPR and 4.80, 5.10, and 5.80 for SAX studies.

EPR study

EPR spectroscopy is useful to provide information on the nature and the structure of the complexes. The EPR spectrum of the Cr–LS system is shown in Fig. 6b. The spectrum of LS alone before Cr(III) treatment, acquired under the same conditions, is also reported (Fig. 6a) in order to check the absence of any ubiquitous metal cations (Fe^{3+}, Mn^{2+} or Cu^{2+}). The EPR spectrum is interpreted based on the spin Hamiltonian:

$$H = \beta(g_x B_x S_x + g_y B_y S_y + g_z B_z S_z) + D[\{S_z^2 - \tfrac{1}{3}S(S+1)\} + (E/D)(S_x^2 - S_y^2)]$$

where S is the electronic spin, D and E/D are the usual axial and rhombic zero-field parameters.[35] The observed g values, $g \sim 4.2$ and ~ 2, are typical of an electronic spin $S = 3/2$, with moderately large zero-field splitting (ZFS) and small rhombicity ($D > h\nu$, $E/D \sim 0$).[36] These parameters are characteristic of a Cr^{3+} ion in an octahedral geometry.[37–39] Moreover, the broad signal at $g \sim 2$ can not be attributed to strong exchange coupled Cr ions (dimeric or polynuclear species) because no Cr–Cr bonds are present according to the EXAFS spectrum (see XAS section). An additional narrow signal is observed at $g = 2.0025$, which corresponds to endogenous semiquinonic species.[40]

X-Ray absorption spectroscopy

The K-edge XANES spectra and their first derivatives for Cr–LS and model compounds are shown in Fig. 7. Oxalate and hydrated nitrate chromium(III) have a slight tetragonally distorted octahedral environment as supposed for the chromium ion in Cr–LS, and has been shown by EPR spectroscopy experiments. A comparison of these XANES spectra reveals that they are almost identical, suggesting strong similarities in the geometry around the metal ion. In XANES spectra of

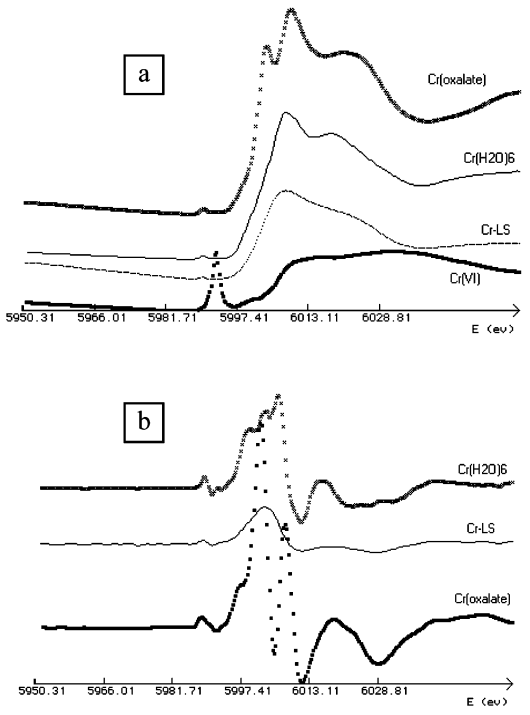

Fig. 7 XANES spectrum of Cr–LS and comparison with those of Cr complexes in various oxidation states (a), and their first derivatives (b).

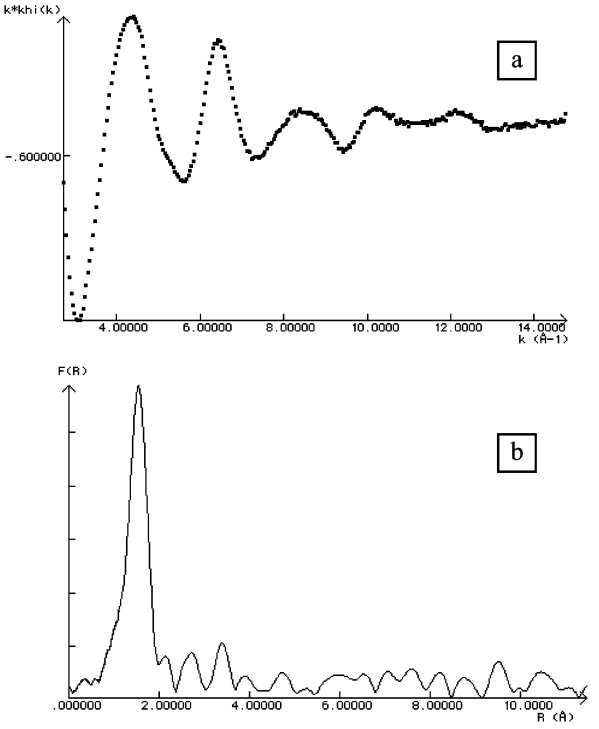

Fig. 8 *k*-Space experimental EXAFS spectrum $k\chi(k)$ *versus* k at the chromium K-edge (a) and the corresponding Fourier transform (b).

Cr(VI) compounds, a prominent pre-edge peak at 5993 eV occurs (Fig. 7a) caused by a bound-state 1s to 3d transition. This transition is forbidden for octahedral $Cr^{III}O_6$ compounds, which have a centre of symmetry, but it is allowed for the non-centrosymmetric tetrahedral $Cr^{VI}O_4$ compounds, due to the mixing of Cr(3d) and O(2p) orbitals.[41] The empty d-orbital ($3d^0$) of Cr(VI) increases the probability of the $1s \rightarrow 3d$ transition, enhancing the pre-edge peak intensity. Nevertheless, before the absorption edge due to $1s \rightarrow 4p$ transitions, at 6003 eV, a small pre-edge feature is present for octahedral Cr(III) at 5990 eV, which is due to $1s \rightarrow 3d$ electronic transitions. Moreover, the intensity of this pre-edge feature is linked to the potential presence of a centre of symmetry, and its intensity is increased by vibronic coupling.[37] So, in our Cr–LS compound, the chromium ion appeared to be essentially in an octahedral environment with an oxidation state +III. The comparison between the XANES spectra of Cr–LS, $Cr(oxalate)_3^{3-}$, and $Cr(H_2O)_6^{3+}$ derivatives shown in Fig. 7b seems to indicate that the Cr^{3+} ion is probably bound to LS through carboxylic moieties, without exclusion of the phenolic groups, in accordance with acid group amounts determined by potentiometric titrations.[3] The chromium coordination sphere is completed with H_2O molecules. Indeed, the Cr–LS derivative XANES spectrum is the sum of the $Cr(oxalate)_3^{3-}\cdot 3H_2O$ and $Cr(H_2O)_6^{3+}$ spectra with approximately 50/50 weighting. This is in accordance with inner-sphere chromium surface complexes.

Fig. 8a shows the $k\chi(k)$ EXAFS function of the Cr–LS compound prepared at pH = 4.80, and Fig. 8b shows the corresponding Fourier transform. The k^3 weighted and phase-corrected Fourier transform function, calculated over the range 2.0–13.0 $Å^{-1}$, gave a main peak at 1.50 Å which arises from first-shell oxygen backscattering. The absence of a significant peak around 2.6 Å allows us to exclude the formation of chromium polynuclear species.[42,43] Quantitative EXAFS results were obtained by fitting the filtered first shell signal (in the 1.20–2.09 $Å^{-1}$ range) to a model of Cr(III) ions co-ordinated to 6 oxygen atoms. Cr–O phase and oxygen amplitude were extracted from the $Cr(oxalate)_3^{3-}\cdot 3H_2O$ reference spectrum. The quality of the fit is shown in Fig. 9. The numerical values thus obtained for the co-ordination number of Cr(III) ions (N) and Cr–O bond length (r) were as follows: $N = 6.13$, r(Cr–O) = 1.90 Å, using $\Delta E = 0.03$ eV. The relative Debye–Waller factor was $\sigma = 0.012$ Å. These pieces of data confirm the results obtained by EPR spectroscopy about the

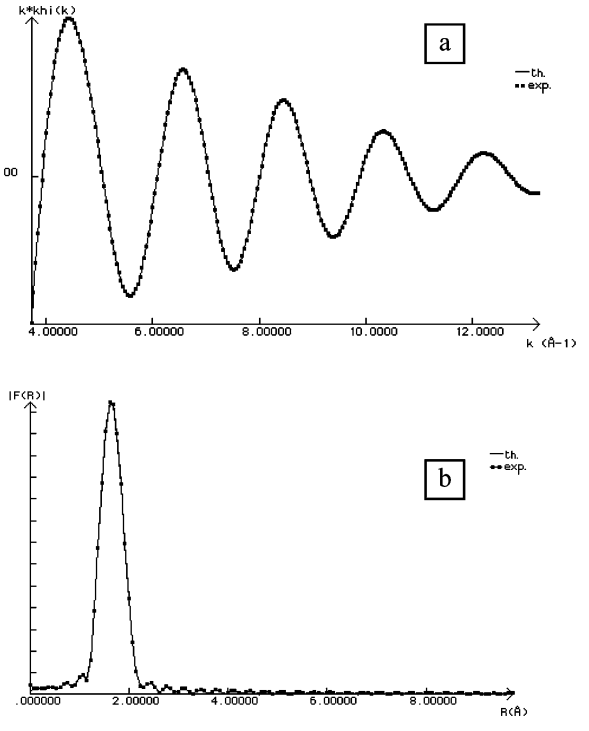

Fig. 9 (a) First-shell fit of the EXAFS function of the Cr–LS system at pH 4.80. (b) Radial structure function of the first shell and its numerical simulation. Experimental first-shell filtered data in the 1.20–2.09 Å range (dotted line), and best fit (solid curve) modeled as Cr–O contributions. Experimental phase and amplitude functions were extracted from the EXAFS spectrum of the $Cr(oxalate)_3\cdot 3H_2O$ reference compound.

nature of the surface complexes. Chromium complexes are isolated species; actually, no Cr atom beyond the first shell of Cr–LS complexes were detected. Both EPR and XAS experiments showed that the chromium is co-ordinated to six oxygen atoms at an average Cr–O distance of 1.90 Å in an octahedral environment. The goodness of the EXAFS fit using the $Cr(oxalate)_3^{3-}\cdot 3H_2O$ phase and amplitude seems to confirm co-ordination through carboxylate functional groups of LS, and that chromium ions are held in inner-sphere complexes in accordance with the XANES study. These results are in good agreement with those obtained from previous spectroscopic studies, from which similar distances and environments are reported.[7,34,44,45] Moreover, the EXAFS spectrum of a Cr–LS sample prepared at pH = 5.80 is completely different from that obtained at pH = 4.80. Indeed, the Cr–O distance obtained in the former case is equal to 2.04 Å (6 neighbouring oxygen atoms), which probably corresponds to chromium hydroxide precipitated at the LS surface. This result is in accordance with surface precipitation compared with surface complexation.

Conclusion

In this work, it was shown that a lignocellulosic substrate extracted from wheat straw is able to bind chromium strongly in aqueous solution. The macroscopic part of this study shows the efficiency of the co-precipitation and precipitation phenomena in removing chromium(III) from a solution. This co-precipitation is known to occur widely in natural systems (*e.g.*, soils) and is used in water treatment plants to remove Cr from industrial effluent waters. However, under our experimental condition (chromium concentration) at pH below 5.20 only sorption reactions occurred. The amount of chromium held, under this condition, on LS is estimated at 4.52 mg g^{-1} (*i.e.* 2.31 μg m^{-2}). The microscopic study by EPR and XAS showed that the sorption of Cr(III) on LS occurs *via* formation of inner-sphere surface complexes. The EXAFS study led to the exact local structure around the metal. The results are consistent with an octahedral configuration, with six Cr–O bond distances at 1.90 Å. The XANES spectrum indicated that the Cr^{3+} ion is bound through carboxylic LS moieties.

However, in natural soil conditions, some hydroxo or polymeric complexes are likely to be formed in addition to chromium(III) complexes. Then, we can expect high retention of this metal, finally yielding to bio-accumulation and, so, pollution of the soil. Nevertheless, in geological systems, surface complexation processes are far more complicated. Indeed, they include reactions with other soil components (metallic oxides, clays, organic substances such as pesticides or industrial wastes, or other metallic cations), and include a kinetic factor.

Acknowledgements

We are grateful to the "Région Champagne-Ardenne" for a grant to K. F. We thank Y. M. Frapart (Université René Descartes, Paris V, UMR 8601, France) for EPR experiments, and P. Beaunier (Université Pierre et Marie Curie, Paris VI, UMR 7609, France) for carrying out the TEM and EDX experiments. The authors also wish to acknowledge S. Belin (Université Paris Sud, LURE, France) for her help in EXAFS and XANES data recording and for helpful discussions.

References

1 K. V. Sarkanen and C. H. Ludwig, *Lignins Occurrence, Formation, Structure and Reactions*, Wiley, New York, 1971.
2 G. Gellerstedt and K. Gustafsson, *J. Wood Chem. Technol.*, 1987, **A24**, 847.
3 P. Merdy, E. Guillon, J. Dumonceau and M. Aplincourt, *Anal. Chim. Acta*, 2002, **459**, 133.
4 A. Marzotto, E. Montoneri, P Savarino, G. Viscardi and U. Croatto, *J. Chem. Biochem. Tech.*, 1993, **48**, 215.
5 S. B. Lalvani, T. S. Wiltowski, D. Murphy and L. S. Lalvani, *Environ. Technol.*, 1997, **18**, 1163.
6 C. Ravat, J. Dumonceau and F. Moteil-Rivera, *Water Res.*, 2000, **34**, 1327.
7 L. Dupont, E. Guillon, J. Bouanda, J. Dumonceau and M. Aplincourt, *Environ. Sci. Technol.*, 2002, **36**, 5062.
8 R. M. Gao, Z. Q. Zhao, Q. Z. Zhou and D. X. Yuan, *Talanta*, 1993, **40**, 637.
9 D. Burrows, *Chromium: metabolism and toxicity*, CRC, Boca Raton, FL, 1993.
10 J. O. Nariagu and E. Nieboer, *Chromium in the nautal and human environments*, Wiley, New York, 1988.
11 S. Peräniemi and M. Ahlgrén, *Anal. Chim. Acta*, 1995, **315**, 365.
12 F. C. Richard and A. C. M. Bourg, *Water Res.*, 1991, **25**, 807.
13 A. R. Walsh, J. O'Halloran and A. M. Gower, *Ecotoxicol. Environ. Safety*, 1994, **27**, 168.
14 R. Leyva Ramos, A. Juarez Martinez and R. M. Guerrero Coronado, *Water Sci. Technol.*, 1994, **30**, 191.
15 P. Merdy, E. Guillon, J. Dumonceau, M. Aplincourt and H. Vezin, *J. Colloid Interface Sci.*, 2002, **245**, 24.
16 (*a*) A. Michalowicz, *Logiciels pour la Chimie*, Société Française de Chimie, Paris, 1991, p. 102; (*b*) A. Michalowicz, *J. Chem. Phys. IV*, 1997, **7**, 235.
17 (*a*) B. K. Teo, *Inorganic Chemistry Concepts, EXAFS: Basic Principles and Data Analysis*, Springer-Verlag, Berlin, 1986, p. 9; (*b*) D. C. Königsberger and R. Prins, *X-ray Absorption Principles, Applications, Techniques of EXAFS, SEXAFS and XANES*, John Wiley, New York, 1988; (*c*) F. W. Lytle, D. E. Sayers and E. A. Stern, Co-Chairmen Report of the International Workshop on Standards and Criteria in X-ray Absorption Spectroscopy, *Physica B*, 1989, **158**, 701.
18 B. Lengeler and P. Eisenberger, *Phys. Rev. B*, 1980, **21**, 4507.
19 P. B. Kaufman, P. Dayanandan, Y. Takeoka, W. C. Bigelow, J. D. Jones and R. Iler, *Silicon and Siliceous Structures in Biological Systems*, ed. T. L. Simpson and B. E. Volcani, Springer, New York, 1981, p. 409.
20 R. S. Rohella, N. Sahoo, S. C. Paul, S. Choudhury and V. Chakravortty, *Thermochim. Acta*, 1996, **287**, 131.
21 D. K. Smith, *Powder Diffr.*, 1998, **13**, 2.
22 J. C. Deelman, *Neues Jahrb. Mineral. Monatsh.*, 1986, 407.
23 H. Graetsch, *Rev. Mineral.*, 1994, **29**, 209.
24 A. Gauthier, S. Derenne, L. Dupont, E. Guillon, C. Largeau, J. Dumonceau and M. Aplincourt, *Anal. Bioanal. Chem.*, 2002, **373**, 830.
25 M. Abou-Sekkina, M. Sakran and A. Saafan, *Ind. Eng. Chem. Prod. Res. Dev.*, 1986, **25**, 676.
26 M. Deraman, S. Zakaria, M. Husin, A. A. Aziz, R. Ramli, A. Mokhtar, M. N. M. Yusof and M. H. Sahri, *J. Mater. Sci. Lett.*, 1999, **18**, 249.
27 K. Csoban, M. Parkanyi-Berka, P. Joo and P. Behra, *Colloids Surf. A*, 1998, **141**, 347.
28 M. Fukushima, K. Nakayasu, S. Tanaka and H. Nakamura, *Anal. Chim. Acta*, 1995, **317**, 195.
29 S. B. Lalvani, A. Hübner and T. S. Wiltowski, *Energy Sources*, 2000, **22**, 45.
30 K. Csoban, M. Parkanyi-Berka and P. Joo, *Magy. Kem. Foly.*, 1996, **102**, 89.
31 A. Kokorevics, J. Gravitis, E. Chirkova, O. Bikovens and N. Druz, *Cellulose Chem. Technol.*, 1999, **33**, 251.
32 D. Rai, B. M. Sass and D. A. Moore, *Inorg. Chem.*, 1987, **26**, 345.
33 L. Spiccia, H. Stoeckli-Evans, W. Marty and R. Giovanoli, *Inorg. Chem.*, 1987, **26**, 474.
34 L. Charlet and A. A. Manceau, *J. Colloids Surf.*, 1992, **148**, 443.
35 A. Abragam and B. Bleaney, *Electron paramagnetic resonance of transition ions*, Oxford University Press, Oxford, 1970.
36 F. E. Mabbs and D. Collison, *Electron paramagnetic resonance of transition metal compounds*, Elsevier, Amsterdam, 1992.
37 D. I. Pattison, A. Levina, M. J. Davies and P. A. Lay, *Inorg. Chem.*, 2001, **40**, 214.
38 N. Shaham, H. Cohen, D. Meyerstein and E. Bill, *J. Chem. Soc., Dalton Trans.*, 2000, 3082.
39 K. P. Bryliakov, M. V. Lobanova and E. P. Talsi, *J. Chem. Soc., Dalton Trans.*, 2002, 2263.
40 E. Guillon, P. Merdy, J. Dumonceau, M. Aplincourt and H. Vezin, *J. Colloid Interface Sci.*, 2001, **239**, 39.

41 M. L. Peterson, G. E. Brown, Jr., G. A. Parks and C. L. Stein, *Geochim. Cosmochim. Acta*, 1997, **61**, 3399.
42 H. Roussel, V. Briois, E. Elkaim, A. de Roy, J. P. Besse and J. P. Jolivet, *Chem. Mater.*, 2001, **13**, 329.
43 L. Rao, Z. Zhang, J. I. Friese, B. Ritherdon, S. B. Clark, N. J. Hess and D. Rai, *J. Chem. Soc., Dalton Trans.*, 2002, 267.
44 A. Manceau, M. L. Schlegei, M. Musso, V. A. Sole, C. Gauthier, P. E. Petit and F. Trolard, *Geochim. Cosmochim. Acta*, 2000, **64**, 3643.
45 P. Merdy, E. Guillon, J. Dumonceau and M. Aplincourt, *Environ. Sci. Technol.*, 2002, **36**, 1728.